Cross-flow fan on multi-dimensional airflow field of air screen cleaning system for rice grain

Yaquan Liang[1], Zhong Tang[1*], Hao Zhang[1], Yaoming Li[1], Zhao Ding[2], Zhan Su[2]
(1. *Key Laboratory of Modern Agricultural Equipment and Technology of Ministry of Education, Jiangsu University, Zhenjiang 212013, Jiangsu, China*;
2. *Key Laboratory of Crop Harvesting Equipment Technology of Zhejiang Province, Jinhua 321017, Zhejiang, China*)

Abstract: With the advancement of agricultural mechanization and the development of combine harvesters, cleaning devices play a very important role in the grain harvesting process. In this study, the DFPF-25 type material floating velocity measuring device was used to measure the suspension velocity of each component of the grain material. Secondly, the DFQX-3 cleaning device was used to conduct the airflow field test, then the fluid simulation of the cleaning shoe was carried out. The results showed that the simulation and experimental results were in a good agreement under the conditions of single fan and double fan. The high-speed flow velocity formed by the double fan system at the tail of the cleaning shoe was 4.76 m/s (simulation) and 4.03 m/s (experiment), which had outstanding cleaning effects on unfilled grains, long stems, and short stems. To sum up, the installation of the cross-flow fan at the rear of the cleaning shoe has a positive effect on the cleaning effect of the combine harvester, and the double-fan cleaning structure composed of the cross-flow fan and the centrifugal fan can significantly improve the cleaning effect.

Keywords: double-fan structure, CFD, cross-flow fan, velocity contour, rice grain
DOI: 10.25165/j.ijabe.20221504.6949

Citation: Liang Y Q, Tang Z, Zhang H, Li Y M, Ding Z, Su Z. Cross flow fan on multi-dimensional airflow field of air screen cleaning system for rice grain. Int J Agric & Biol Eng, 2022; 15(4): 223–235.

1 Introduction

In recent years, agricultural mechanized harvesting has developed rapidly around the world. The main working parts of the combine harvester include the cutting device, transport device, threshing device, and cleaning system. The cleaning system can directly affect the impurity rate and loss rate of the harvesting operation, which shows that research on the cleaning system is very necessary. Air-screen cleaning is the main form of the current cleaning system, which is mainly composed of cleaning fans, vibrating screens, and grain conveying augers. The airflow condition of the cleaning shoe is used as the research object to study the performance of the cleaning system.

The cleaning system relies on the airflow of the fan and the reciprocating movement of the vibrating screen to complete the separation and cleaning of the materials discharged from the threshing device so that the grains can fall into the grain conveying auger below and the surplus is discharged from the tail of the cleaning shoe. Efforts to make all the grains fall below and efforts to keep the surplus from falling below are two important indicators of the cleaning system. Different scholars have conducted research from different directions. The positional relationship and motion parameters between the cleaning fan and the vibrating screen have always been an important research direction. The research parameters of the fan include fan speed, fan installation inclination, and fan outlet shape[1-3]. Chai et al.[4] conducted three-factor and three-level simulation tests on the inlet installation angle, blade curvature, and blade inlet curvature of the centrifugal fan, and the outlet wind speed and direction were proved to be affected by these factors. The parameters of the vibrating screen include the size of the vibrating screen, the period of vibration, the amplitude of vibration, and the inclination of the vibrating screen[5,6]. The chaffer has been widely used in the vibrating screen of the cleaning system, which means that the spacing and opening of the screen have become important parameters that affect the work of the vibrating screen.

The interaction between air flow and material is the operating mechanism of the cleaning system. The complex structure inside the cleaning system usually requires certain means to obtain airflow data. Ueka et al.[7] used paper image velocimetry and laser Doppler velocimetry to measure the flow velocity of the cleaning air. However, high-speed imaging and laser speed measurement have high test costs and conditions, which has not become a common research method. The method of combining simulation and experiment has become a mature method for research on cleaning systems[8,9]. Computational Fluid Dynamics (CFD) simulation plays an important role in analyzing the airflow field of cleaning shoe. The gas-solid coupling of the Computational Fluid Dynamics-Discrete Element Method (CFD-DEM) can simulate the characteristics of material movement in the cleaning system.

Some scholars have found the best parameter settings and improved the cleaning system through multi-factor experiments. However, the combine harvester needs to deal with a more complex working environment, and changes in the feed volume and

Received date: 2021-06-13 **Accepted date:** 2022-05-28
Biographies: Yaquan Liang, Master candidate, research interests: intelligent harvesting machinery, Email: 823389273@qq.com; **Hao Zhang**, Master candidate, research interests: intelligent harvesting machinery, Email: 1160387587@qq.com; **Yaoming Li**, PhD, Professor, research interests: intelligent harvesting machinery, Email: ymli@ujs.edu.cn; **Zhao Ding**, PhD, research interests: intelligent harvesting machinery, Email: dingzhao0806@foxmail.com; **Zhan Su**, PhD, research interests: intelligent harvesting machinery, Email: sz_627@126.com.
***Corresponding author: Zhong Tang**, PhD, Professor/Doctoral Supervisor, research interests: intelligent harvesting machinery. School of Agricultural Equipment Engineering, Jiangsu University, Zhenjiang 212013, Jiangsu, China. Tel: +86-511-88797338, Email: tangzhong2012@126.com.

material characteristics would directly affect the airflow-material action law of cleaning shoe. Automatic control was used by some scholars in the parameter control of the cleaning system. Through the fuzzy control algorithm under big data, real-time adjustment of multiple parameters is realized to meet the actual working conditions[10,11]. Liang et al.[12] developed a fuzzy control system, which can monitor the sieve loss of grains through the monitoring device in the cleaning system. Based on fuzzy control, the main working parameters of the combine harvester could automatically adapt to changes in crops and the environment, thereby improving the cleaning performance.

The effect of optimizing the cleaning system on the structural parameters to improve the cleaning effect is limited. Although many scholars have optimized the structure of different types of harvesters, they have not caused significant changes in the airflow law of the cleaning shoe. Different cleaning shoe structures were gradually proposed to improve the cleaning effect. In this process, the fan and the cleaning screen are still important entry points. The arrangement of multi-air duct centrifugal fans and multi-layer vibrating screens has been studied to improve the performance of the cleaning system[13]. Gebrehiwot et al.[14,15] used CFD and hot wire anemometer measurements to study the flow structure and performance of a cross-low fan (CFF) used for grain cleaning. Cross-flow fans were considered for cleaning systems. The volute and the position of the air outlet of the cross-flow fan have been studied to analyze the influence on the air flow, but there is no complete study on the effect of the cross-flow fan on the cleaning result.

In summary, although there are many studies on combine harvester cleaning, they mainly focus on the research of cleaning fans and vibrating screens. Aiming at the problem of poor distribution of airflow field in the cleaning device of the combine harvester, this study proposed cross-flow fan as an auxiliary fan for shoe cleaning. Firstly, the flow field characteristics and material suspension velocity of the traditional single-fan cleaning device were measured, and the cleaning defects were analyzed. Secondly, use the double fan test and simulation to analyze the airflow field of the system after adding the cross-flow fan, to explore the positive effect of the cross-flow fan on the cleaning shoe. The research of this study has important application significance for the design and optimization of the combine harvester cleaning device.

2 Materials and methods

2.1 Experimental design for determination of grain suspension speed

In vertical systems containing materials and fluids, when the fluid moves upward at a speed less than the free settlement speed of the material, the material would fall. When the fluid moves upward at a speed greater than the free settlement speed of the material, the material would rise. When the fluid moves upward at a speed equal to the free sedimentation speed of the material, the material would be in a state of equilibrium, and the speed of the fluid at this time is called the free suspension speed of the material. The suspension speed is an important parameter when calibrating the performance of the cleaning system. The fluid velocity of the air flow field needs to be between the grain and the impurities to achieve the cleaning effect[16].

The equipment for measuring the grain suspension speed in this study included the DFPF-25 material floating speed measuring device (Figure 1), pressure velocity meter, tape measure, electronic caliper, etc. The material is the cleaning material that enters the cleaning shoe during the operation of the combine harvester (Figure 1), and the variety is Zhendao No. 10. The materials mainly include full grains, shriveled grains, long stems (50-120 mm), short stems (20-50 mm), long grass, light waste (husks and broken leaves), etc.

Figure 1 DFPF-25 material floatation-specific measuring device and material

The DFPF-25 type material floating specific measuring device is 2.2 m in length, 0.9 m in width, and 3.0 m in height. The supporting power is 5.5 kW, the floating speed is less than or equal to 25 m/s, and the fan speed is 1000 r/min. The diameter of the small end of the tapered tube is 81 mm, and the taper of the tapered tube is 5.5°. Randomly pick 100 grains from the harvester's grain bin, and measure their geometry and quality. Using calipers to measure its length, width, and thickness, the average length of rice grains is 7.28 mm; the average width is 3.36 mm, and the average thickness is 2.51 mm. The average thousand-grain weight of rice

grains is 24.3 g.

Each material was designed to repeat the floating speed test 10 times. Because the tested materials were mostly irregular shapes, the accurate suspension position could not be obtained in the airflow of the tapered pipe. During the test, read the upper and lower limits of the position of the material in the tapered tube, and calculate the suspension speed range through the calculation equation. The speed of the small end of the cone observation tube was the average of four measuring points. The air velocity calculation equation for any end surface is Equation (1)[17].

$$V_i = \frac{V_1 D_1^2}{(D_1 + 2L\sin\varphi)^2} \quad (1)$$

where, V_i is the air velocity of any section of the cone observation tube, m/s; D_1 is the diameter of the small end of the cone observation tube, m; L is the position of the material floating up and down in the cone tube, m; V_1 is the airflow velocity at the small end of the cone-shaped observation tube, m/s; φ is the taper of the cone-shaped tube. After completing the suspension speed test, the experimental data will be imported into SPSS software for the single-sample *K-S* test.

2.2 Airflow field test design in the cleaning shoe

After the threshing drum completes the threshing, the output is not evenly distributed on the plane of the vibrating screen, and the material distribution law is high in the front and low in the back. During the operation of the cleaning system, the vibrating screen can evenly shake the effluent to the screen surface, and the light materials are screened to the tail of the screen surface[18]. Larger impurities are discharged through the tail screen to the cleaning shoe. The fan plays an auxiliary role in this process, and the flow field speed does not need to reach the suspension speed of these materials.

The centrifugal fan is mainly composed of an impeller and a casing. The air entering the impeller rotates with the impeller and is discharged out of the casing under the action of centrifugal force. At this time, a certain degree of vacuum is generated at the center of the impeller, and the surrounding air is continuously sucked into the impeller. When the air flows in the centrifugal fan, the external mechanical work is transferred to the air by the impeller, so that it has certain dynamic pressure energy and static pressure energy. When the air with a very high velocity leaves the impeller and enters the volute with a gradually increasing cross-sectional area, part of its velocity energy can be converted into static pressure energy, and finally discharged outside the machine to form a high-speed airflow[19].

The cross-flow fan is forced to rotate in the impeller due to the airflow with larger pressure head loss and lower efficiency. However, the cross-flow fan has the characteristics of simple structure, straight and uniform wind, high dynamic pressure coefficient, and low noise.

The structure of the cross-flow fan is composed of an impeller, volute, and volute tongue. The impeller is multi-blade, long cylindrical, one part is open, and the other part is surrounded by a volute. When the impeller rotates, the airflow enters the cascade from the open part of the impeller, passes through the interior of the impeller, and is discharged into the volute from the other side of the cascade to form a working airflow. The flow coefficient of the cross-flow fan is approximately proportional to the size of the impeller diameter. In a certain shape and size, the characteristic curve of the cross-flow fan will be affected by the shape and size of the volute[20]. The impeller of the cross-flow fan adopts forward arc blades. The parameters of the cross-flow fan are shown in Table 1.

Table1 Parameters of the cross-flow fan

Parameter	Value
Inlet installation angle of impeller	60°
Outlet installation angle	25°
Outer diameter of the impeller	150 mm
Length of the blade chord	25 mm
Number of blades	20
Length of the impeller	900 mm
Volute tongue gap	7.5 mm

As the main component of the cleaning system, the parameters of the vibrating screen and the fan directly affect the cleaning effect. Chaffer and other sieve faces are shown in Figure 2. The chaffer with the adjustable opening is used as the main type in the cleaning system. The opening of the screen is designed to be between 0-36 mm, and the screen surface inclination α=(±10)°[20]. In order to make up for the uneven distribution of the axial airflow of the centrifugal fan, the method of connecting two fans in series is used to solve this problem, and the inclination angle of the air outlet of the centrifugal fan is 25°[21].

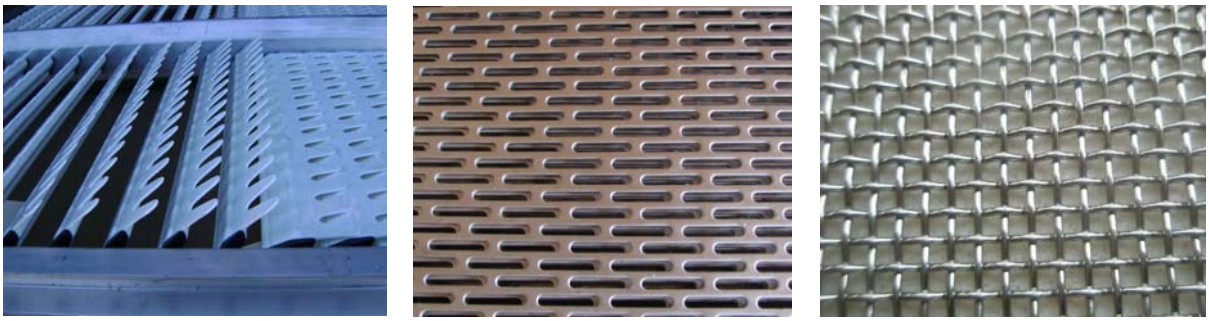

a. Chaffer b. Perforated sieve c. Braided sieve

Figure 2 Different sieve classifications

Combine harvesters for the rice, wheat, rape, and other crops mostly use a fan and double-layer vibrating screen structure. Using the different aerodynamic characteristics of materials to carry out airflow cleaning, this kind of cleaning mechanism has the advantages of mature technology and convenient maintenance. Based on the above cleaning principle, the DFQX-3 cleaning system was used to clean the air flow field test in the shoe. The test bench is shown in Figure 3.

The overall dimensions (length×width×height) of the DFQX-3 cleaning system are 4.8 m×2.5 m×4.0 m, the cleaning capacity is 3 kg/s, and the supporting total power is 27.6 kW. When the combine harvester performs rice harvesting operations, the working parameters of the main components that affect the airflow field are set as listed in Table 2.

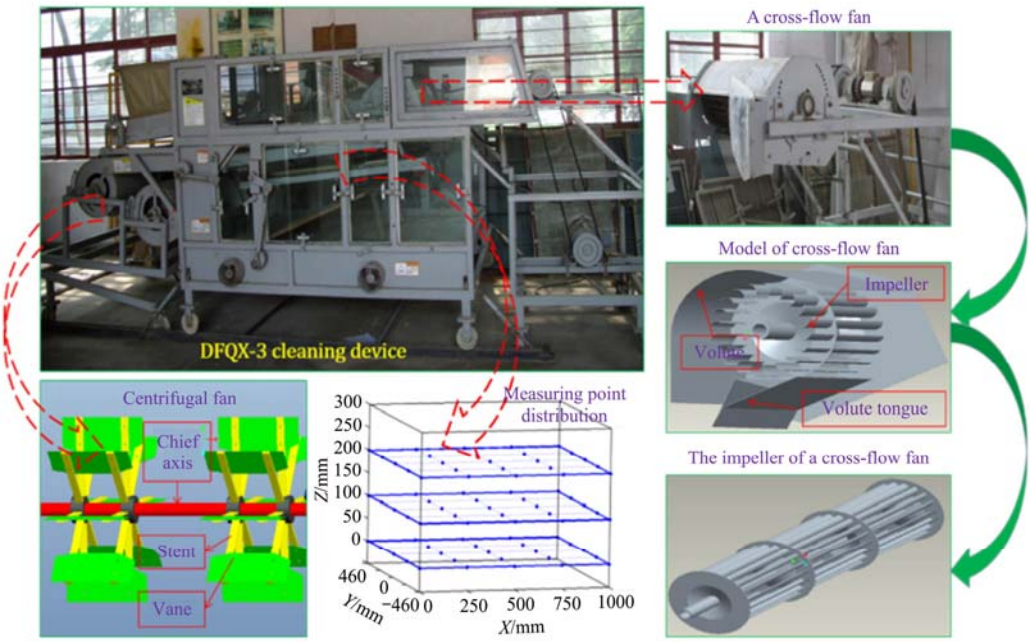

Figure 3 Main structure of the DFQX-3 cleaning system test bench

Table 2 Working parameters of the DFQX-3 cleaning system

Component	Main parameter value
Centrifugal fan	Position: horizontal 0-400 mm, vertical 0-300 mm Speed: 600-1300 r/min Inclination angle of the air outlet: 10°-30°
Cross flow fan	Position: horizontal 0-400 mm, vertical 0-300 mm Speed: 600-1300 r/min
Vibrating screen	Vibration frequency: 0-7 Hz Installation angle: (±10)° Screen length 800-1600 mm
Jitter board	Amplitude: 5-20 mm

The structure of the DFQX-3 cleaning system is mainly composed of a shaking plate, a centrifugal fan, a screen box, an upper vibrating screen, a lower vibrating screen, a cleaning shoe, a cross-flow fan, a grain receiving tank, a frame, a transmission system, and sensors. A speed sensor is installed on the power input shaft of a centrifugal fan, a cross-flow fan, and a double-layer vibrating screen, and an angle measurement sensor is installed on the centrifugal fan. The centrifugal fan, double-layer vibrating screens, and cross-flow fan are driven by speed-regulating motors, and the speed can be adjusted. The centrifugal fan is two identical centrifugal fans connected in series coaxially, and the two fans are separated by 100 mm.

In the experiment, the inclination angle of the centrifugal fan was set to 25°, the speed was 950 r/min, 1050 r/min[22], and the double-layer chaffer was selected, and its size was 1200 mm×1200 mm. Use the smart anemometer to measure the wind speed at different locations in the space under the condition of no protruding objects. The room temperature during the test was 22°C. Five horizontal measuring points are set uniformly in the *X*-direction, the coordinates are 0, 250 mm, 500 mm, 750 mm, and 1000 mm, respectively. Five horizontal measurement points are uniformly set in the *Y*-direction, the coordinates are −460 mm, −230 mm, 0, 230 mm, and 460 mm. Set three levels of horizontal measurement points in the *Z*-direction, the coordinates are 0, 100 mm, and 200 mm.

After completing the collection of the airflow field velocity of the cleaning shoe, the discrete data points in the three-dimensional space are subjected to nonlinear regression based on the least squares method through Matlab. Then use the color to express the value of the flow rate. In addition, use the contour function in Matlab to draw isokinetic lines of different planes.

2.3 Simulation design of the airflow field of cleaning shoe

The fluid simulation method based on Fluent is widely used in the research of cleaning systems. The airflow conditions in the cleaning shoe can be comprehensively evaluated through simulation, which helps to analyze the distribution law of the airflow field. Based on the experimental platform to perform isometric modeling and set the simulation parameters, the airflow simulation of the cleaning shoe is designed to be compared with the experiment. The global characteristics of the cleaning shoe can be presented through simulation, and the airflow data can be obtained through simulation in areas that are difficult to test through experiments.

The RNG k-ε turbulence model was used in the simulation of the cleaning shoe[23]. Compared with the standard k-ε turbulence model, the former considers the influence of eddy currents on turbulence in the calculation process, which is beneficial to improving the accuracy of airflow calculation in cleaning shoes. The vortex phenomenon would appear in the complex cavity structure[24]. However, based on this fluid model, it is necessary to deal with the walls in contact with the fluid, and a roughness of 0.05 is set in the boundary conditions of the flow field wall[25].

The structural design and parameter optimization of the cleaning shoe are the main ways to improve the cleaning effect, and this study focused on the structural design. The addition of a cross-flow fan at the tail is an innovative design used in the cleaning system of the combine harvester. The addition of a cross-flow fan is used as an important link in the cleaning simulation to explore the performance characteristics of the dual-fan cleaning shoe structure. By designing the working conditions of the cleaning system with only centrifugal fans and the working conditions of the auxiliary centrifugal fans of the cross-flow fans at different wind speeds, the influence of multi-fan operations on the cleaning effect was studied.

The test measured the average wind speed of the two fans at different speeds. The centrifugal fan was installed at the lower part of the front end of the cleaning screen, and the inclination

angle of the air outlet was set to 25°. The rotational speed of the centrifugal fan was designed to be 850, 950, 1050, 1150, and 1250 r/min. The corresponding average wind speeds are 8.47, 9.06, 11.02, 11.15, and 12.43 m/s. The cross-flow fan plays the role of inhaling the cleaning materials, and the air inlet is the main research object. The wind speed was measured at 50 points at the air inlet, and the average wind speed at different rotation speeds was obtained. The wind speed of the cross-flow fan was designed to be 950, 1150, and 1250 r/min, and the corresponding average wind speed is 3.92, 4.40, and 5.93 m/s. The wind speed of the air inlet is bound to change due to the structure of the centrifugal fan and the cleaning shoe. Using the wind speed of the air inlet of the cross-flow fan as a boundary condition would cause the simulation to be distorted.

In fact, the cross-flow fan would form a negative pressure at the inlet during the working process, and the negative pressure phenomenon can play a role in suction during the working process[26,27]. This work feature can be considered for inhaling and expelling the body from the light impurities in the cleaning shoe. The inlet negative pressure value of the cross-flow fan is calculated based on the Bernoulli equation[28] (Equation (2)).

$$P_1+\frac{1}{2}\rho v_1^2=P_2+\frac{1}{2}\rho v_2^2 \tag{2}$$

$$P_1=0.6025\times(v_2^2-v_1^2)\ \ P_1=0.6025\times(v_2^2-v_1^2) \tag{3}$$

where, P_1 is the inlet pressure of the cross-flow fan, Pa; P_2 is the outlet pressure of the cross-flow fan, Pa; ρ is the fluid density, kg/m^2. When air is regarded as an incompressible fluid, the density is regarded as 1.205 kg/m^2. v_1 and v_2 are the inlet wind speed and outlet wind speed of the fan, respectively, m/s.

The air outlet of the fan is considered to be the standard atmospheric pressure. When P_1 and P_2 are used as the relative static pressure for calculation, P_2=0 Pa. After bringing the density of air into the equation, the calculation result of the inlet negative pressure is shown in Equation (3). The outlet wind speed is required to be tested to calculate the inlet wind pressure of the fan, and an anemometer is also used to test the outlet wind speed of the fan at different speeds. Table 3 lists the calculation of the wind speed at the air inlet, the air at the air outlet, and the negative pressure at the air inlet of the cross-flow fan.

Table 3 Main boundary condition parameters of the fan

Fan speed /r·min^{-1}	Centrifugal fan outlet wind speed/m·s^{-1}	Inlet wind speed of cross-flow fan/m·s^{-1}	Outlet wind speed of cross-flow fan/m·s^{-1}	Negative pressure at the inlet of cross-flow fan/Pa
950	9.062	3.92	7.53	−24.90
1150	11.15	4.40	9.68	−44.79
1250	12.43	5.93	11.88	−63.84

Under the same wind speed, the outlet wind speed of the cross flow fan is less than that of the centrifugal fan, which is consistent with the performance comparison of the two fans. The cross-flow fan could form a relatively stable flow area and wind speed distribution curve, but the kinetic energy of the outlet wind speed at the same speed and power is lower than that of the centrifugal fan. The inlet negative pressure of the cross-flow fan is −24.90 Pa, −44.79 Pa, and −63.84 Pa at three wind speeds. As the fan speed increases, the negative pressure level at the outlet gradually increases, and the corresponding adsorption capacity should also increase.

3 Results

3.1 Material suspension velocity measurement

The floating speed of each cleaning material was tested 10 times under the DFPF-25 type material floating specific measuring device. The specific data are listed in Table 4.

Table 4 Material floating speed and distribution parameters

Parameter		Saturated grain	Unsatisfied grain	Long stem	Short stem	Light impurity
Material floating speed/m·s^{-1}	Teste 1	6.359	5.341	5.456	5.766	2.590
	Test 2	6.732	4.734	6.295	6.043	2.513
	Test 3	6.193	4.938	4.914	5.976	2.976
	Test 4	6.850	4.552	6.8	4.797	3.106
	Test 5	7.682	5.923	7.108	5.947	2.709
	Test 6	7.194	4.328	5.547	4.850	2.513
	Test 7	7.117	5.393	5.812	4.120	2.737
	Test 8	6.426	6.547	6.276	4.392	2.638
	Test 9	6.679	4.657	6.903	6.127	2.701
	Test 10	6.717	5.673	6.290	4.862	3.022
Mathematical expectation (μ)		6.537	4.265	5.573	4.300	2.751
Standard deviation (σ)		0.314	0.387	0.519	0.528	0.213

The test data was further imported into SPSS for analysis. It could be found that the five data items all obey the normal distribution with a significance level of 0.05 under the single-sample *K-S* test[29]. From this, the average value and floating deviation of different material floating speeds are also obtained. Due to the normal distribution, the "3σ criterion" was followed to obtain the upper limit and lower limit of the floating speed of each material, as shown in Figure 4.

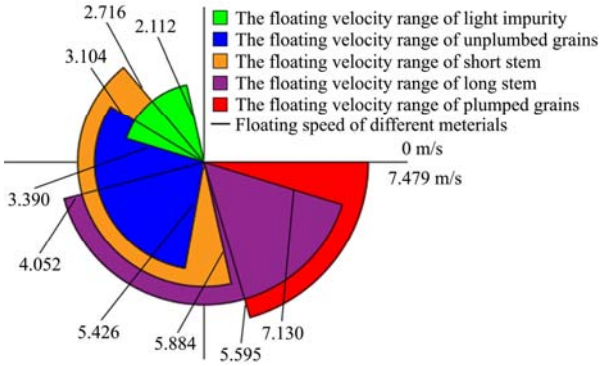

Figure 4 Floating speed range of five materials (m/s)

It can be seen that only the floating speed of long stems and the suspension speed of full grains overlap, which can easily lead to bad conditions such as dirty cleaning or increased loss rate. The maximum speed of 7.479 m/s was obtained in the measurement of the suspension speed of plumped grain, while the lower limit of the suspension speed of light impurities of 2.112 m/s was observed in the experiment. The floating speed of unplumbed grain and light impurities were small, and this part was not considered to be the focus of the selection. However, the content of light trash, which was different from the grains, would still affect the cleaning rate.

Although the average value and standard deviation of the floating speed of short stems were large, considering the "Pauta criterion" under the normal distribution, the maximum value has not reached the lower limit of the floating speed of full grain. Controlling the air velocity of cleaning shoes between 5.884-7.130 m/s would not cause the loss rate to increase theoretically. Based on this, the cleaning performance under different fan combinations could be further studied.

3.2 Single fan airflow field test

By adjusting the speed regulating motor of the centrifugal fan, the fan speed could be controlled at 950 r/min and 1050 r/min. Use an anemometer to measure wind speed at the measuring point, and visualize the experimental data through software[30]. Constant

velocity lines and cloud diagrams can intuitively express the law of airflow above the screen surface in different sections. The cross-sectional data in three dimensions was considered for drawing the air velocity cloud diagram, which could intuitively analyze the airflow laws in different directions of the cleaning system. Based on the coordinate systems established by the velocity measurement points, the *X*-*Y* plane and the *X*-*Z* plane were considered to be the main research content. This is because the cleaning system has a symmetrical structure along the $Y=0$ section.

When the rotational speed of the centrifugal fan was 950 r/min, the airflow field distribution in the measurement space is shown in Figure 5. The symmetrical law of airflow along $Y = 0$ was observed, which was consistent with the symmetrical structure in the cleaning shoe. The arrangement of the double centrifugal fans did not make the 100 mm gap in the middle appear low wind speed, on the contrary, the airflow wind speed is higher near the center line.

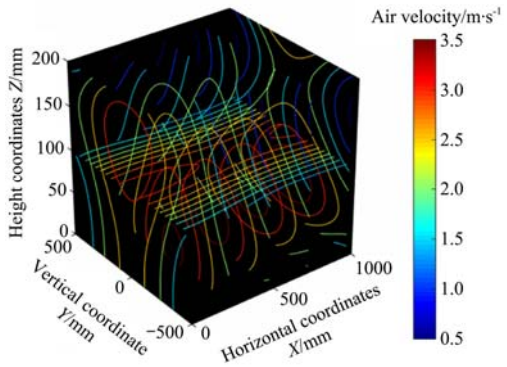

Figure 5 Constant velocity line diagram of air flow field at 950 r/min

As the spatial coordinates shift to both sides along the *Y*-direction, the airflow velocity gradually decreases. The air distribution near the screen surface can be more clearly observed in Figure 6. The same symmetrical distribution law exists on the *X*-*Y* plane, and the wind speed on both sides was as low as 1.0 m/s. The fan was located at the front end of the vibrating screen so that the front end wind speed could reach 3.5 m/s. The flow velocity distribution near the screen surface was consistent with the falling distribution of the material in the threshing device, which was beneficial to the vibrating screen to effectively screen the material and prevent material accumulation.

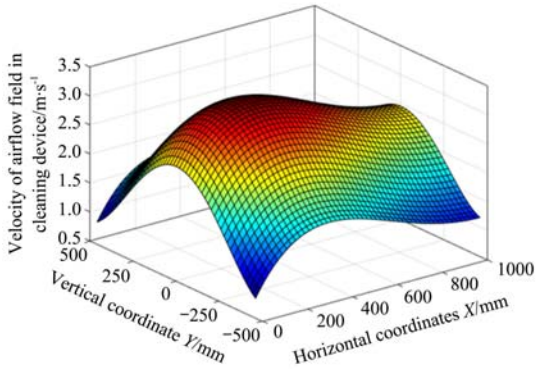

Figure 6 Air velocity distribution diagram in the $Z=0$ horizontal plane

The flow field rule of the centrifugal fan at the speed of 1050 r/min for cleaning shoes was similar to that at the level of 950 r/min, except that the wind speed level at the air inlet was higher. The constant velocity line contains an increased area, which was manifested as an increase in the high-speed airflow area in the middle and a more uniform airflow in this area. The attenuation of the air flow after passing through the vibrating screen did not show the expected increase in air flow on the screen surface, and the attenuation effect of the vibrating screen on the air flow was not a proportional decrease.

Multiple planes were selected to further analyze the airflow conditions above the screen surface of the cleaning shoe. This was also the main area where the material was cleaned after being discharged from the threshing device and entering the cleaning system. Under the wind speed level of the centrifugal fan of 950 r/min, the cross-sections in all directions were analyzed. The distribution of the four plane constant velocity lines is shown in Figure 7. The $X=0$ section had a relatively high wind speed area at the height of $Z=150$ mm, and the contour value was 2.93 m/s, while the near-screen surface showed a lower wind speed between 1.10-2.41 m/s. Part of the airflow from the air outlet of the fan directly bypassed the front transverse edge of the vibrating screen and directly acts on the top of the screen surface, causing this phenomenon. This showed that although it was a single-channel fan, the airflow would split in the actual process of drying. One part passes between the screens and the other part flows directly above the screen surface by the fan.

The plane $X = 1000$ showed the air flow at the tail of the vibrating screen. A high-velocity area was observed near the screen surface in Figure 7b, with the highest air velocity reaching 3.28 m/s. The same symmetrical distribution was observed in the two cross-sections $X=0$ and $X=1000$. The low wind speed in the areas closed to both sides also showed up. There was a significant difference in the output of the threshing drum in the *X*-direction but not in the *Y*-direction. The flow velocity distribution in the *Y*-direction of the cleaning system would directly affect the cleaning effect of the material. Through the $Z=100$ plane, it could be seen that the airflow difference between the middle and both sides was about 1.39 m/s, and the flow velocity in the middle was twice the flow velocity on both sides. Significant horizontal uneven distribution is a problem that needs to be analyzed and resolved.

The difference in flow velocity in the *Z*-direction could be observed in Figure 7c through the $Y=0$ plane. The high flow rate near the screen surface could assist the vibrating screen to effectively separate the materials during throwing and achieve a good cleaning effect. However, the flow velocity in the upper plane was lower than the flow velocity near the screen surface under the same coordinates, and the difference was between 0.93-1.40 m/s. Improving the airflow above the screen surface to a higher level helps to classify and screen the material in the initial stage of falling, and significantly reduces the workload of the cleaning system.

Some phenomena and problems could be found in the experiment. The centrifugal fan could effectively act on multiple areas in the cleaning shoe, but the vibrating screen would significantly suppress the air flow above the screen surface. The uneven distribution of the air flow in the axial direction of the fan is amplified above the screen surface, and the unevenness of the wind speed may even form a negative vortex in the cleaning shoe. When the airflow of the fan reaches the plane above the cleaning shoe through a long path, the airflow speed dropped significantly. Therefore, improving the airflow field above would effectively improve the working effect of the cleaning system.

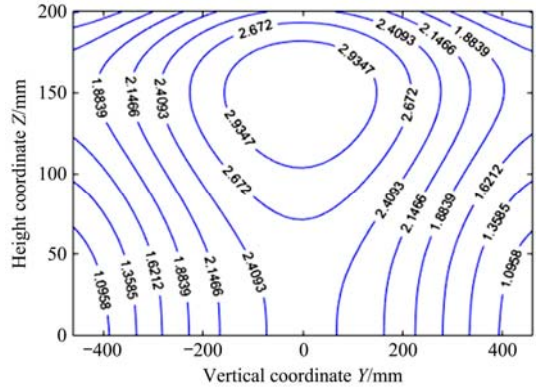

a. Section X=0 mm

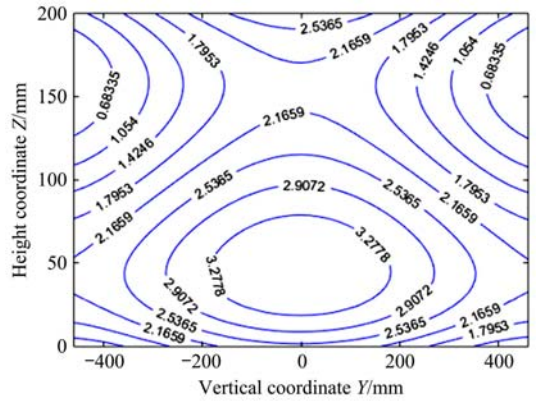

b. Section X=1000 mm

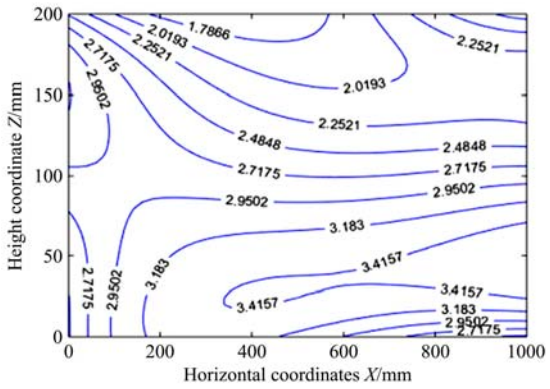

c. Section Y=0 mm

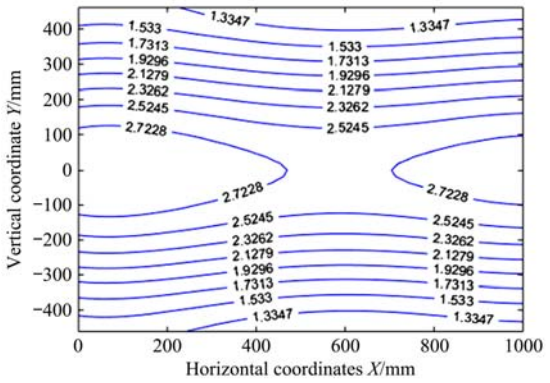

d. Section Z=100 mm

Figure 7 Sectional constant velocity line

3.3 Simulation of airflow field in cleaning shoe

3.3.1 Simulation of single fan airflow field

In the modeling process, considering the installation position of the cleaning screen and the opening of the screen surface, 30°, 45°, and 60° were used as three levels to study the airflow conditions in the cleaning shoe under different screen inclination angles. In order to simplify the model and make the simulation results easier to converge, the driving mechanism and assembly structure of the cleaning system were omitted. The screen size was 1200 mm×1200 mm. The inclination angle of the screen surface was 10°.

The simulation boundary condition settings include the wind speed of the air inlet was 10.426 m/s, the inclination angle of the chaffer was 45°, the fluid outlet type is set to pressure outlet, and the pressure was 0 Pa. The airflow in the cleaning shoe is shown in Figure 8. Obvious air velocity differences were observed at the front and rear ends of the cleaning screen. It was clear that the air velocity at the front of the screen surface could reach 10.41 m/s, while the air velocity at the tail of the screen surface was 1.65 m/s or even lower. The difference in air velocity above and below the screen surface could also be observed, and the attenuation of the airflow by the cleaning screen was observed to be consistent with the experiment in the simulation. The flow direction of the airflow could be more clearly observed in the cloud diagram of the cross-section of the cleaning shoe.

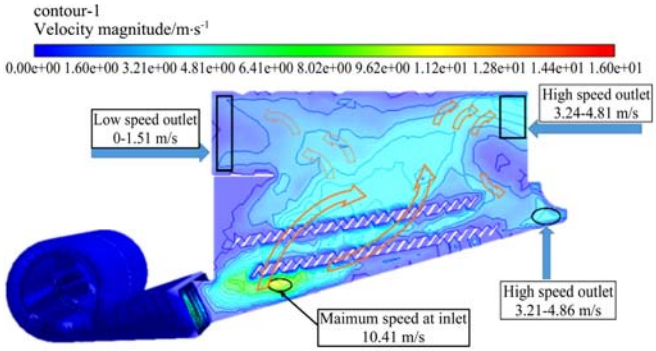

Figure 8 Cross-sectional airflow cloud diagram of a single fan

Another negative phenomenon was manifested in the simulation process. It could be seen that a downward velocity vector appears above the tail of the cleaning screen. The downward airflow would reduce the cleaning effect at the tail of the cleaning screen. Improving the cleaning effect of the tail screen was considered to be an effective way to improve the cleaning performance. The lower air velocity at the far screen surface was observed in the simulation results.

The three sets of airflow distribution cloud diagrams of the simulated Y=0 section were intercepted as shown in Figure 9. The airflow conditions were significantly different. When the screen is 30°, the inclination angle between the outlet of the centrifugal fan and the relative included angle of the screen was small, and the airflow direction was hardly affected by the screen surface. However, significant airflow intensity attenuation could be observed under this condition. The 45° inclination angle was considered to be able to form a good airflow environment in the cleaning shoe, and a larger high-speed airflow area was observed above the vibrating screen, which means that a more uniform airflow field is formed in the cleaning shoe. Comparing the above two conditions, the 60° inclination angle of the screen showed a bad airflow field condition, and part of the airflow flows out through the outlet above the vibrating screen. There was a vortex area at the front end of the screen surface, which would cause material accumulation during operation. At the same time, a low wind speed area was observed above the front end of the cleaning screen, which is not conducive to the uniform distribution of materials on the screen surface.

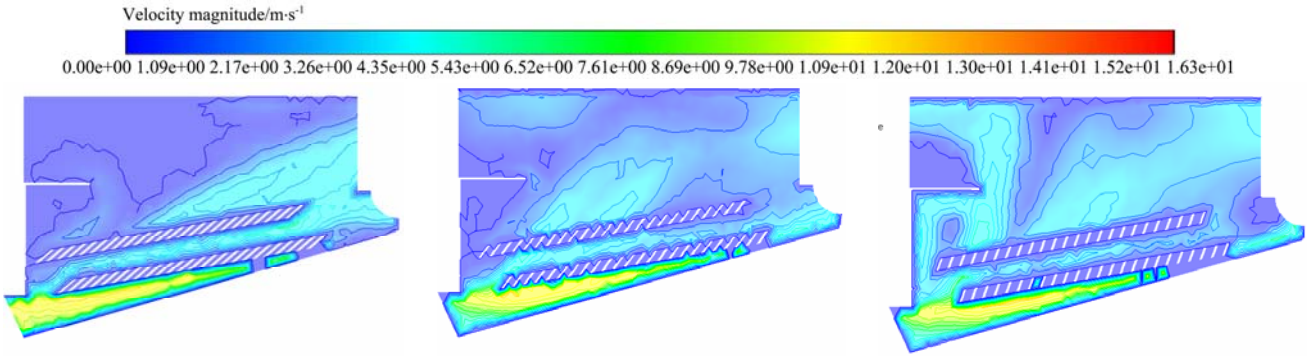

a. Sieve opening 30° b. Sieve opening 45° c. Sieve opening 60°

Figure 9 Airflow simulation cloud diagram of different screen openings

3.3.2 Simulation of the airflow field of dual fans

Based on a single fan simulation test, the opening of the cleaning screen was set to 45°. The other boundary conditions remained unchanged, and the negative pressure of the air inlet was set at the position of the cross-flow fan at the tail of the cleaning shoe. The negative pressure value of the air inlet of the cross-flow fan was used as a variable in the dual-fan simulation test, and the airflow state in the cleaning shoe was analyzed by observing the simulation results.

When the centrifugal fan and the cross-flow fan worked together, the inlet negative pressure of the cross-flow fan was set to −24.9 Pa. The appearance of a negative pressure changed the airflow pattern in the cleaning shoe. The airflow cloud diagram was shown in Figure 10. It could be observed from the *X*-*Z* plane that the airflow above the rear half of the vibrating screen is larger than the first half. The regular isokinetic line distribution showed that a better airflow was formed at the tail of the cleaning shoe, which was significantly different from the structure of the single-fan cleaning shoe. The air velocity in the $Y=0$ plane was less than the air velocity in $Y=\pm 460$. The air outlet of the centrifugal fan is two rectangular outlets of 550 mm×240 mm, while the air inlet of the cross-flow fan runs through the *Z*-direction of the cleaning shoe. The airflow intensity law in the *Z*-direction was still dominated by the centrifugal fan. The phenomenon that the wind speed on both sides of the fan is significantly higher than in the middle is clearly observed in the *X*-*Z* plane cloud chart and the *X*-*Z* cloud chart, which is consistent with the analysis result of the *X*-*Z* plane cloud chart.

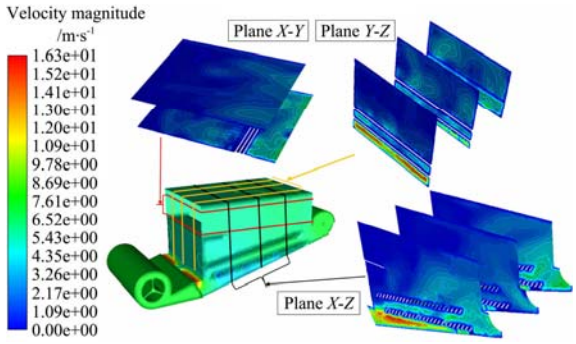

Figure 10 Cross-sectional cloud diagram of the airflow simulation for cleaning shoe with dual fans

The phenomenon of increased wind speed of cleaning shoes could be shown in the cloud diagram in the same direction, especially the position of wind speed at the outlet of the centrifugal fan for cleaning shoes. The boundary conditions of the centrifugal fan outlet had not changed, but the outlet wind speed ranges from 10.09-12.50 m/s, even reaching 13.3 m/s near the screen surface. As the only variable, the setting of the cross-flow fan was believed to have caused an increase in the outlet wind speed of the centrifugal fan. The setting of the cross-flow fan was believed to improve the airflow conditions in the cleaning shoe. As shown in Figure 11, the density and arrows in the speed vector diagram represented the wind speed value. The main movement direction of the airflow wad from the centrifugal fan into the cleaning shoe was passing through the double-layer vibrating screen and blowing to the tail screen outlet. The direction of the velocity vector was all upwards except for a small part of the vortex area. These chaotic vortices are distributed on the front side of the vibrating screen, which was considered to not affect the cleaning effect.

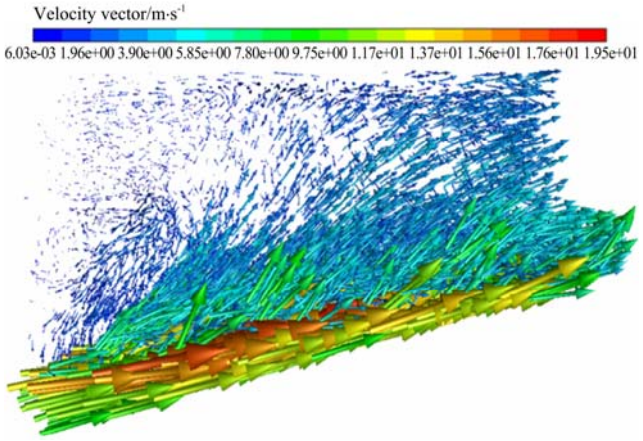

Figure 11 Airflow velocity vector diagram of the cleaning shoe with dual fans

Compared with the airflow field of a single fan, significant changes had taken place in the airflow field, and a better flow field was observed in the airflow cloud diagram. In order to study whether the distribution law of the airflow would change with the change of the negative pressure at the inlet of the cross-flow fan, more control experiments were designed to further study the influence of the cross-flow fan on the air flow field of the cleaning shoe. The inlet negative pressure levels of −24.9 Pa, −44.76 Pa, −63.84 Pa, and −100 Pa are designed for testing.

As the negative pressure value at the outlet of the cross-flow fan increased, the high-speed airflow area in the cleaning shoe tended to increase, two high airflow regions were shown on both sides of the X=50 plane, The plane cleaning shoe simulation airflow speed of X=50 is listed in Table 5. At three different rotational speeds, the airflow speed is between 0.70-3.81 m/s. When the negative pressure at the outlet of the cross-flow fan was increased to 100 Pa, there was still an obvious boundary between the two high airflow areas, and the increase in wind speed was

observed but not obvious. In addition, the air velocity showed the same law under the four boundary condition levels.

Comparing the average air velocities above and below the chaffer, a clear difference can be seen in Table 5. However, almost all airflow velocities did not increase significantly when the inlet negative pressure of the cross-flow fan was increased.

Table 5 *X*=50 plane cleaning shoe simulation airflow speed

Inlet negative pressure /Pa	Upper chaffer maximum speed /m·s^{-1}	Upper chaffer minimum speed /m·s^{-1}	Upper chaffer average speed /m·s^{-1}	Upper chaffer maximum speed /m·s^{-1}	Upper chaffer minimum speed /m·s^{-1}	Under chaffer average speed /m·s^{-1}
−24.90	3.66	0.85	2.75	12.60	4.65	6.02
−44.79	3.75	0.70	2.60	13.30	4.68	6.22
−63.84	3.81	0.86	2.87	12.91	4.50	6.07
−100.00	3.88	0.90	3.22	12.70	4.71	6.37

The cross-flow fan could significantly increase the area affected by the airflow in the cleaning shoe. The increase of the wind-receiving area above the screen surface directly affected the operation effect of the cleaning system, especially the cleaning ability of lightweight materials and the obvious improvement. The increase in air velocity under the vibrating screen was a notable feature, which means that the centrifugal fan can be set to a lower speed to achieve the predetermined cleaning effect. The change in the rotational speed of the cross-flow fan had little effect on the air flow field in the cleaning shoe. Larger negative pressure can lead to an increase in the high-speed airflow area for cleaning shoe. However, the change in the negative pressure of the fan inlet caused by the increase of the fan speed was limited, and the improvement of the airflow field in this way had great limitations.

3.4 Airflow field test of double fans

3.4.1 Influence of cross-flow fan on air flow field

The simulation of the cleaning shoe verified the positive effect of the cross-flow fan on the cleaning system. The dual-fan airflow test was designed to verify the simulation results under the same conditions. The fan speeds of 1150 r/min and 1250 r/min of the cross-flow fan were set in the dual fan air flow field test. Since the pre-test showed that the rotational speed of the centrifugal fan did not have a significant effect on the law of the airflow field, the wind speed of the centrifugal fan was set to a fixed value of 10.426 m/s.

The speed of the cross-flow fan was adjusted to 1150 r/min, and then an anemometer was used to capture the wind speed at the measuring point in the cleaning shoe. The distribution of constant velocity lines on the vertical plane of the screen Y=0 is shown in Figure 12a. Two high-speed airflow regions were observed on the right and bottom left of the image. These two positions correspond to the air inlet of the cross-flow fan and the air outlet of the centrifugal fan, and the maximum wind speed was 3.63 m/s and 4.76 m/s respectively. Compared with the airflow speed under the rotating speed of other cross-flow fans, the increase in the rotating speed would not change the distribution characteristics of the airflow field.

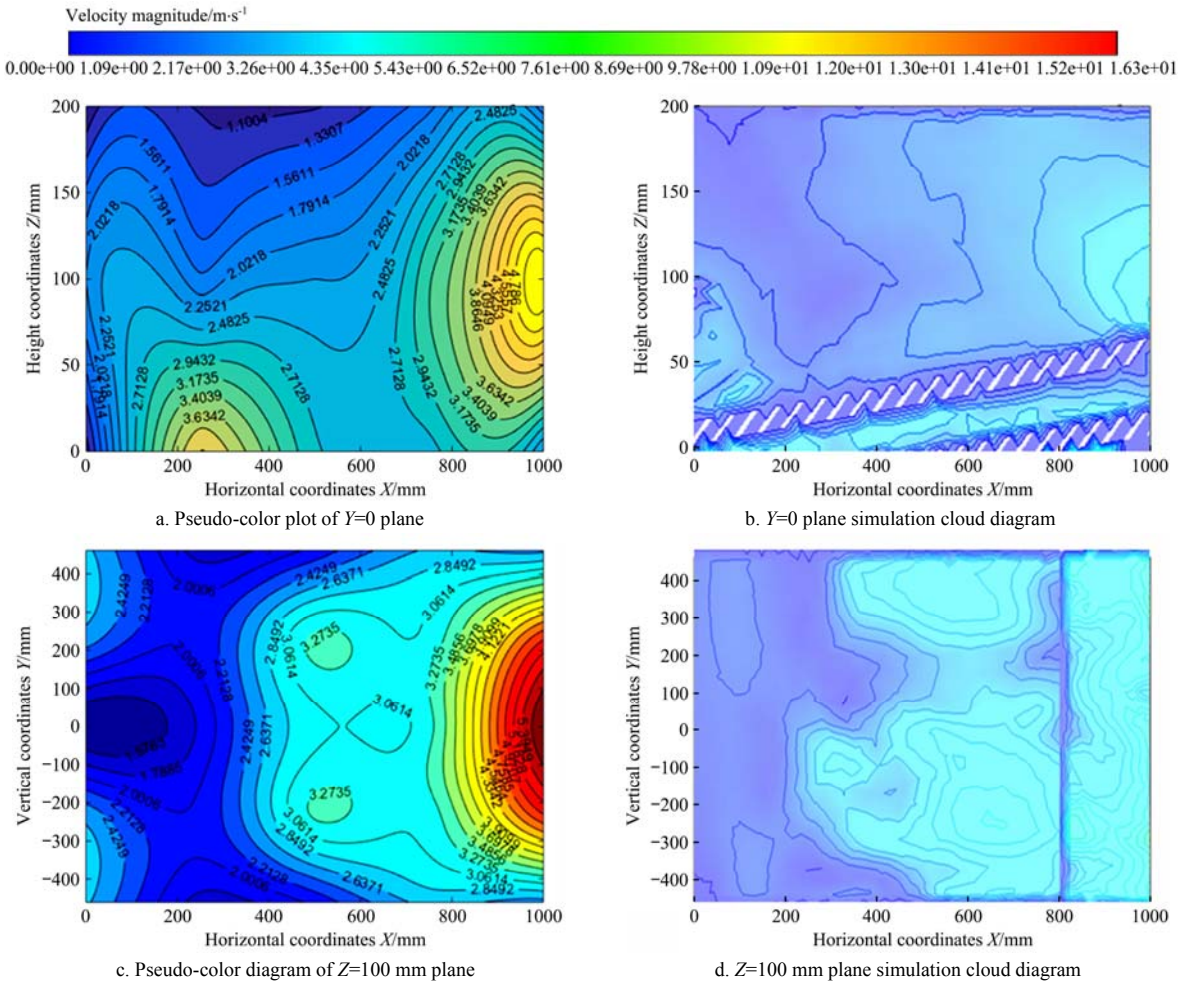

a. Pseudo-color plot of Y=0 plane

b. Y=0 plane simulation cloud diagram

c. Pseudo-color diagram of Z=100 mm plane

d. Z=100 mm plane simulation cloud diagram

Figure 12 Comparison of experimental pseudo-color image and simulated cloud diagram

The experimental phenomenon of the $Y=0$ plane was consistent with the simulation results. Under the same boundary conditions, two high-speed airflow regions are also observed in Figure 12b. The maximum wind speed was 2.98 m/s and 4.03 m/s.

Compared with the experiment, the errors were 0.65 m/s and 0.73 m/s, respectively. In comparison, the test constant velocity line was more uniform, which showed that in the actual cleaning process, the airflow in the cleaning shoe was stable, and less turbulent airflow and vortex flowed out of the cleaning system during the operation. The turbulence in the simulation test made the wind speed at the same location smaller than the test wind speed. On the Y=0 plane, the test verified the correctness of the simulation well in general.

When the rotational speed of the cross-flow fan was 1250 r/min, the airflow velocity on the Z=100 mm plane was shown in Figure 12c. The simulated cloud image under the same boundary conditions is shown in Figure 12d. 5.39 m/s and 5.63 m/s were the inlet wind speed of the cross-flow fan measured by the test and the inlet wind speed of the simulation test respectively. The simulation error was only 4.4%. This also showed the correctness and accuracy of the method of simulating the influence of the cross-flow fan on the airflow of the cleaning shoe with the negative inlet pressure as the boundary condition. Another similar phenomenon could be observed in the two pictures. Two sub-high wind speed regions appeared near Y=±200 mm and X=300 mm, which was on the left side of the inlet of the cross-flow fan. Under the action of the centrifugal fan, the cleaning shoe airflow was almost symmetrically distributed along the Y=0 plane, while the cross-flow fan can only affect this law in the area near the air inlet. The centrifugal fan still plays a leading role in the airflow field in the cleaning system.

3.4.2 Determination of cleaning effect of double fans

Since the floating speed of each material presents a normal distribution trend, its probability density function and distribution function are shown in Equation (4) and Equation (5).

$$f(x)=\frac{1}{\sqrt{2\pi}\sigma}e^{-\frac{(x-\mu)^2}{2\sigma^2}},\ (-\infty<x<+\infty) \tag{4}$$

$$F(x)=\int_{-\infty}^{x}f(t)\mathrm{d}t=\frac{1}{\sqrt{2\pi}\sigma}\int_{-\infty}^{x}e^{-\frac{(t-\mu)^2}{2\sigma^2}}\mathrm{d}t \tag{5}$$

where, x is the sample parameter; μ is the sample mean; σ is the sample variance. Since unsatisfied grains, long stems, short stems, and light impurities are all impurities, the probability of these four materials being discharged out of the field by the airflow is taken as the average value of the cleaning rate of the cleaning system. The probability of full grain being discharged off the field should be counted as the loss rate.

Based on the airflow velocity at each point in the airflow field under different conditions obtained in the experiment, the airflow velocity could be obtained by substituting the airflow velocity into Equation (2) to obtain the cleaning probability and the loss probability at each point in the airflow field. When the rotational speed of the centrifugal fan was 950 r/min and the rotational speed of the cross-flow fan was 1250 r/min, the images of the cleaning rate and the failure rate in the cleaning shoe are shown in Figure 13.

It could be seen from Figure 13a that no obvious loss rate would be caused at each spatial point in the cleaning shoe, and the loss is only 1.00% in the case of the largest loss. From Figure 13b, it could be found that the maximum point of impurities removal rate when the combined fan is at Z=100 appeared on the X-Y plane, which was consistent with the law of the two-dimensional contour map under the combined fan.

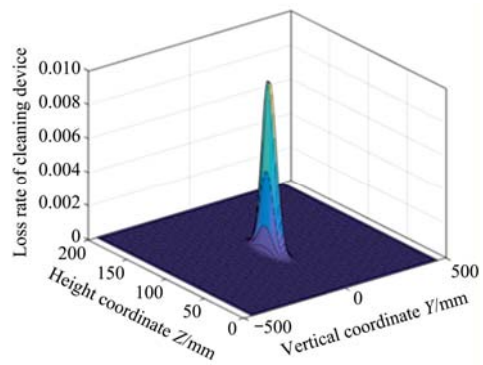

a. Loss rate function

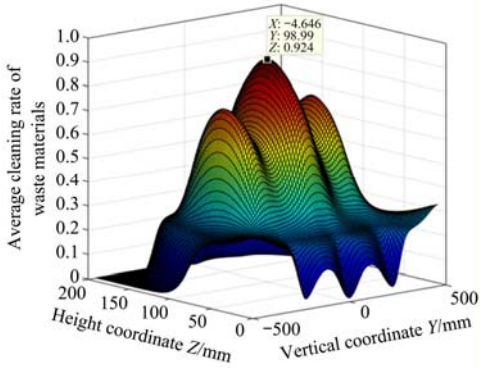

b. Cleaning rate function

Figure 13 Image of the loss rate and the cleaning rate of dual fans

The impurity rate and loss rate data of each component of the cleaning system are shown in Table 6. When the rotational speed of the centrifugal fan was 950 r/min, the average cleaning rate would continue to increase as the rotational speed of the cross-flow fan increased. It could be seen that the cleaning efficiency on the experimental bench is lower than the actual cleaning system, especially when there is only a centrifugal fan, the average cleaning rate was only 24.56%. When the cross-flow fan was added, the cleaning rate of unsatisfied grains increased from 0.18% to 68.33%, and the cleaning rate of short stems increased from 1.41% to 61.15%. As the speed of the cross-flow fan increased from 950 r/min to 1050 r/min, the cleaning rate of long stems significantly improved, but it was only 26.24%. The continuous increase in the wind speed of the cross-flow fan did not make the long-stems cleaning rate reach a high level, and it was only 69.81% when the speed was 1250 r/min.

Table 6 Loss rate and cleaning rate under different working conditions

Terms	Cross flow fan speed (Centrifugal fan 950 r/min)				
	0 r/min	950 r/min	1050 r/min	1150 r/min	1250 r/min
Loss rate	1.47×10^{-27}	4.43×10^{-14}	1.49×10^{-11}	1.14×10^{-5}	1%
Selection rate-unsatisfied grains	0.18%	68.33%	99.25%	99.92%	100%
Selection rate-long stems	1.96×10^{-6}	1.81%	26.24%	46.63%	69.81%
Selection rate-short stems	1.41%	61.15%	95.71%	98.81%	99.78%
Selection rate-light impurities	96.66%	100%	100%	100%	100%
Average cleaning rate	24.56%	57.82%	80.31%	86.34%	92.40%

When the centrifugal fan and the cross-flow fan were combined in series, increasing the speed of the cross-flow fan would still not have much impact on the loss rate, but it could

significantly improve the cleaning efficiency of the device. Increasing the speed of the cross-flow fan from 950 r/min to 1050 r/min would greatly improve the average cleaning rate. After further increasing the speed to 1250 r/min, the influence of the loss rate cannot be ignored, but the average cleaning rate reached 92.40%. At this time, the main material that cannot be effectively cleaned was long stems.

In fact, it was difficult to clean long stems directly out of the cleaning shoe through the airflow. The reciprocating motion of the chaffer can screen the long stems to the end of the screen and exclude the body. The airflow field could reduce the resistance of large-volume impurities such as long stems in the movement process and effectively prevent the screen surface from clogging. For large-volume materials, the suspension velocity has a large numerical value span, and it is inaccurate to judge the cleaning rate only by the airflow velocity. However, the increase in the cleaning rate of long stems could qualitatively show that the cross-flow fan has a positive effect on the cleaning of this part of the impurities.

4 Discussion

The intensification process of grain harvesting has developed rapidly in recent years, resulting in the need to design a larger feed rate for the combine harvester to meet the harvesting efficiency. Increased material would use more resistance to the airflow field in the cleaning shoe. It is difficult for the airflow of the centrifugal fan to reach the rear of the device, which would directly cause the high impurity content of the grain. Therefore, it is necessary to explore the wind speed distribution of the air flow in the space of the traditional fan screen cleaning device and find out the law and deficiency of the air flow field distribution. Taking the airflow field in the cleaning shoe as the dependent variable, a cleaning structure with better performance is designed.

In this study, the airflow field of a single-fan cleaning device was measured, and some phenomena and problems could be found in the working process. Centrifugal fans could be effective in cleaning multiple areas within the shoe, but the presence of a vibrating screen can significantly dampen the airflow intensity above the screen surface[31]. The uneven distribution of the airflow in the axial direction of the fan was amplified above the screen surface, and the unevenness of the wind speed could even form a negative eddy current in the cleaning shoe. When the air flow of the fan traveled a long way to the upper plane of the cleaning shoe, the air flow speed decreased. Improving the airflow field above would effectively improve the working effect of the cleaning device. On the other hand, there are often more impurities behind the cleaning shoe[32], and it is very meaningful to consider measures to improve the airflow field at the rear so that the impurities could be discharged more easily.

A CFD simulation experiment was carried out on the distribution of the airflow field inside the single-fan cleaning shoe. On the one hand, the results confirmed the consistency between the test and the simulation, and bad airflow field distribution appeared at the rear and the top of the cleaning shoe. On the other hand, the opening of the sieve was found to have a significant effect on the airflow field. In fact, when there is a relative angle between the screen and the centrifugal fan, the screen will have a divergent effect on the wind speed, which can be observed in three simulation tests. The kinetic energy loss of the airflow is manifested in the friction with the walls of the vibrating screen. The change of the airflow direction and coverage of the fan will also change the cleaning effect. Under the condition of a 45° sieve inclination angle, the airflow condition of the cleaning shoe was more suitable for grain cleaning. Selecting this condition as quantitative for further simulation was considered to be able to obtain a better cleaning effect.

The wind speed at the air inlet of the cross-flow fan was smaller, but the wind speed distribution in the axial direction was more uniform than that of the centrifugal fan. When the material enters the cleaning device, the vertical speed was small, and changing the initial transverse speed would have a significant impact on the position where the material finally falls on the vibrating screen. In this paper, a cross-flow fan is installed above the tail of a traditional cleaning shoe to optimize the airflow field. From the results of the simulation and experiment, the distribution of the flow velocity cloud map was better than that of a single fan. Although the cross-flow fan cannot provide strong airflow, it could significantly change the airflow above the vibrating screen.

There are differences in the suspension speed of different materials, and they showed different movement modes and movement paths after entering the cleaning device. Only plump kernels were expected to fall through the double-layer vibrating screen into the feeding auger below. Other impurities need to be discharged from the rear of the vibrating screen under the action of the vibrating screen and the fan[33]. The use of a vibrating screen could make full use of the mechanical properties of different materials to screen materials of different volumes and shapes, which would not be limited to the suspension speed of materials[34]. The movement state of the material under different conditions could be obtained by analyzing the airflow field law of the single fan and the double fan.

As shown in Figure 14a, when only a centrifugal fan was used, the lightweight surplus could be blown to the rear of the fan by the airflow. Other materials move under the front of the vibrating screen and close to the surface of the screen due to the high suspension speed. The air velocity near the screen surface was 3.42 m/s. In the single fan test, the reciprocating motion of the vibrating screen could achieve the effect of screening and cleaning materials. However, when the material moves close to the sieve surface, the movement distance is limited, and part of the stems would fall into the grain conveying auger along with the grains, thereby increasing the impurity content. The air velocity in the space above the screen surface is small, and the airflow difference of 0.93-1.40 m/s in the Z-direction makes it difficult to separate the impurities in the tail screen[35].

The dual fan structure provides a uniform airflow field and a high-speed airflow area at the rear of the cleaning shoe. As shown in Figure 14b, as the centrifugal fan and the cross-flow fan are used at the same time, then the movement mode of the material behind the cleaning shoe changes. The cleaning effect of light materials has been improved because the airflow velocity at the front and rear ends of the cleaning shoe is not significantly reduced at the height of $Z=200$ mm. Obvious changes in the material behind the screen surface could be predicted in the dual fan systems. The mathematical expectation of the suspension velocity of unsatisfied grains and short stems was 4.265 m/s and 4.300 m/s, which are very close to the velocity value of 4.270 m/s in the high-speed airflow zone at the tail. In the simulation, the airflow level behind the cleaning shoe was between 4.360-5.450 m/s. The movement path of the material is increased under the action of the airflow, which makes less material fall into the grain conveying auger during the vibration of the vibrating screen. The cross-flow

fan can actively absorb light impurities, short stems, and unsatisfied grains. Better cleaning effects could be predicted through analysis.

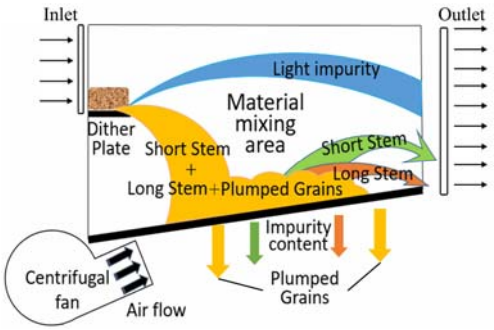

a. Schematic diagram of material trajectory under a single fan

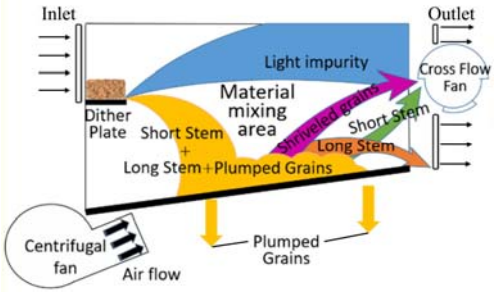

b. Schematic diagram of material trajectory under dual fans

Figure 14 Schematic diagram of materials in cleaning shoe

In order to meet different cleaning needs, there have been many achievements in the design and research of centrifugal fans and vibrating screens. It was an exploratory study to install a cross-flow fan at the rear of the cleaning shoe to optimize the airflow field and improve the cleaning effect in this paper. Airflow field tests and CFD simulations have preliminarily proved the positive effect of the cross-flow fan. The cleaning tests of rice and wheat will be the next important stage of this research.

In this study, through a series of airflow field tests and CFD simulations, it had been clarified that the effect of the cross-flow fan on the airflow in the cleaning chamber is local. In this experiment, it was found that the speed of the fan has little effect on the airflow field. But in future tests, in order to ensure the accuracy of the test results, the fan speed will be still an important variable. In addition, the humidity of the material has a significant impact on the cleaning effect. In future research, the effect of material cleaning and impurity content will be the focus of research.

5 Conclusions

This study presented research on the use of cross-flow fans in combine harvester cleaning devices. Experiments and simulations of a single fan showed that the screen inclination has a significant effect on the airflow distribution. The airflow was more suitable for grain cleaning under the condition of 45° screen inclination in three sets of simulations. The increase of the centrifugal fan speed had little effect on the airflow speed above the cleaning shoe. In the dual-fan test, the cross-flow fan made the airflow field at the rear of the cleaning shoe uniform and the high wind speed area increased, which had a better effect on the material moving to the rear of the vibrating screen. Coupling the measured grain suspension velocity with the experimental wind velocity showed that the maximum loss rate of the double-fan cleaning device is less than 1.00%. The double fan structure has an outstanding cleaning effect on underfilled grains, long stalks, and short stalks. Adding a cross-flow fan at the rear of the cleaning shoe could significantly improve the cleaning effect. The results of this study is verified that adding a cross-flow fan at the end of the cleaning shoe has a positive effect, which provides a feasible way for the performance optimization of the cleaning device of the combine harvester.

Acknowledgements

This work was financially supported by the National Natural Science Foundation of China (Grant No. 52175235), the Key Laboratory of Modern Agricultural Equipment and Technology (Jiangsu University), the Ministry of Education (MAET202109), the Key Laboratory of Crop Harvesting Equipment Technology of Zhejiang Province (Grant No. 2021KY02), and the Jiangsu Province "Six Talents Peak" High-level Talent Project (GDZB-085). The data used to support the findings of this study are available from the corresponding author upon request.

[References]

[1] Tang Z, Li Y, Li X Y, Xu T B. Structural damage modes for rice stalks undergoing threshing. Biosystems Engineering, 2019; 186: 323–336.

[2] Dai F, Song X F, Shi R J, Zhao W Y, Guo W J, Zhang Y. Migration law of flax threshing materials in double channel air-and-screen separating cleaner. Int J. Agric & Biol Eng, 2021; 14(3): 92–102.

[3] AL Aasmi A, Li J H, Hamoud Y A, Lan Y B, Alordzinu K E, Appiah S A, et al. Impacts of slow-release nitrogen fertilizer rates on the morpho-physiological traits, yield, and nitrogen use efficiency of rice under different water regimes. Agriculture, 2022; 12(1): 86. doi: 10.3390/agriculture12010086.

[4] Chai X Y, Xu L Z, Sun Y X, Liang Z W, Lu E, Li Y M. Development of a cleaning fan for a rice combine harvester using computational fluid dynamics and response surface methodology to optimise outlet airflow distribution. Biosystems Engineering, 2020; 192: 232–244.

[5] Xu L Z, Li Y, Chai X Y, Wang G M, Liang Z W, Li Y M, et al. Numerical simulation of gas-solid two-phase flow to predict the cleaning performance of rice combine harvesters. Biosystems Engineering, 2020; 190: 11–24.

[6] Zhang N, Fu J, Chen Z, Chen X G, Ren L Q. Optimization of the process parameters of an air-screen cleaning system for frozen corn based on the response surface method. Agriculture, 2021; 17(8): 794. doi: 10.3390/agriculture11080794.

[7] Ueka Y, Matsui M, Inoue E, Mori K, Okayasu T, Mitsuoka M. Turbulent flow characteristics of the cleaning wind in combine harvester. Engineering in Agriculture, Environment and Food, 2012; 5(3):102–106.

[8] Chen M, Chen Z, Gong M, Tang Y P, Liu M L. CFD-DEM-VDGM method for simulation of particle fluidization behavior in multi-ring inclined-hole spouted fluidized bed. China Particuology, 2021; 57(4): 112–126.

[9] Wang C, Li H W, He J, Wang Q J, Lu C Y, Yang H Y. Optimization design of a pneumatic wheat-shooting device based on numerical simulation and field test in rice-wheat rotation areas. Agriculture, 2022; 12(1): 56. doi: 10.3390/agriculture12010056.

[10] Craessaerts G, Baerdemaeker J D, Missotten B, Seays W. Fuzzy control of the cleaning process on a combine harvester. Biosystems Engineering, 2010; 106(2): 103–111.

[11] Liu Q Y, Chen S, Zhou L, Tao Y, Tian J Y, Xing Z P, et al. Characteristics of population quality and rice quality of semi-waxy japonica rice varieties with different grain yields. Agriculture, 2022; 12(2): 241. doi: 10.3390/agriculture12020241.

[12] Liang Z W, Li Y M, Xu L Z. Grain sieve loss fuzzy control systems in rice combine harvesters. Appl. Sci., 2018; 9(1): 114. doi: 10.3390/app9010114.

[13] Liang Z W, Xu L Z, De Baerdemaeker J, Li Y M, Saeys W. Optimisation of a multi-duct cleaning system for rice combine harvesters utilising CFD and experiments. Biosystems Engineering, 2020; 190: 25–40.

[14] Gebrehiwot M G, Baerdemaeker J D, Baelmans M. Numerical and experimental study of a cross-flow fan for combine cleaning shoe. Biosystems Engineering, 2010; 106(4): 448–457.

[15] Gebrehiwot M G, De Baerdemaeker J, Baelmans M. Effect of a cross-flow opening on the performance of a centrifugal fan in a combine harvester: Computational and experimental study. Biosystems

Engineering, 2010; 105(2): 247–256.
[16] Tang Z, Liang Y Q, Wang M L, Zhang H, Wang X Z. Effect of mechanical properties of rice stem and its fiber on the strength of straw rope. Industrial Crops and Products, 2022; 180: 114729. doi: 10.1016/j.indcrop.2022.114729.
[17] Liu Q Y, Chen S, Zhou L, Tao Y, Tian J Y, Xing Z P, et al. Characteristics of population quality and rice quality of semi-waxy japonica rice varieties with different grain yields. Agriculture, 2022; 12(2): 241. doi: 10.3390/agriculture12020241.
[18] Xu L Z, Li Y, Li Y M, Chai X Y, Qiu J. Research progress on the cleaning technology and equipment of grain combine harvester. Transactions of the CSAM, 2019; 50(10): 1–16. (in Chinese)
[19] Ding W S. Analysis of internal flow field for a three-stage centrifugal fan under various operating conditions. The Journal of Engineering, 2019; 2019(13): 328–334.
[20] Badretdinov I, Mudarisov S, Khasanov E, Nasyrov R, Tuktarov M. Operation technological process research in the cleaning system of the grain combine. Journal of Agricultural Engineering, 2021; 52(2): 1129. doi: 10.4081/jae.2021.1129.
[21] Tang Z, Li Y M, Li H C, Xu L Z, Zhao Z. Analysis on the eddy current of the air-and-screen cleaning system. Transactions of the CSAM, 2010; 41(12): 62–66. (in Chinese)
[22] Lin T, Zargar O A, Lin K Y, Juiña O, Sabusap D L, Hu S C, et al. An experimental study of the flow characteristics and velocity fields in an operating room with laminar airflow ventilation. Journal of Building Engineering, 2020; 29: 101184. doi: 10.1016/j.jobe.2020.101184.
[23] Pan Y, Chen C. Exploring the relationship between particle deposition and near-wall turbulence quantities in the built environment. Building and Environment, 2021; 196: 107814. doi: 10.1016/j.buildenv.2021.107814.
[24] Akram M A, Khushnood S, Tariq S L, Nizam L A; Ali H M. The effect of grid generated turbulence on the fluidelastic instability response in parallel triangular tube array. Annals of Nuclear Energy, 2021; 158(3): 108245. doi: 10.1016/j.anucene.2021.108245.
[25] Tang Z, Li Y, Zhao H, Mei R, Hui Y. Screening model and optimization of grains group by queuing theory on air-And-screen cleaning system. International Agricultural Engineering Journal, 2017; 26(3): 103–111.
[26] Moosania M, Zhou C, Hu S T. Aerodynamics of a partial shrouded low-speed axial flow fan. International Journal of Refrigeration, 2021; 130: 208–216.
[27] Tiwari J, Kim K, Zhang M, Yeom T. Experimental study on convection heat transfer enhancement of channel-flow with piezoelectric fan. Heat Transfer Engineering, 2022; 2027105. doi: 10.1080/01457632.2022.2027105
[28] Zhou S Q, Deng H Y, Ma Y, Zhang S C. Investigation on the performance of forward bending fan. International Journal of Turbo & Jet-Engines, 2019; 36(2): 207–217.
[29] Zhao Q, Jiang H B, Chen B, Wang C, Xu S Z, Zhu J H, Chang L. Research on state of health for the series battery module based on the Weibull distribution. Journal of The Electrochemical Society, 2022; 169(2): 020523. doi: 10.1149/1945-7111/ac4f21.
[30] Meng F N, Dong Q L, Wang P F, Wang Y. Multiobjective optimization for the impeller of centrifugal fan based on response surface methodology with grey relational analysis method. Advances in Mechanical Engineering, 2014; 2014: 614581. doi: 10.1155/2014/614581.
[31] Wang H, Zhang H, Hu X W, Luo M H, Wang G J, Li X T, Zhu Y X. Measurement of airflow pattern induced by ceiling fan with quad-view colour sequence paper streak velocimetry. Building and Environment, 2019; 152: 122–134.
[32] Liang Z W, Li Y M, De Baerdemaeker J, Xu L Z, Saeys W. Development and testing of a multi-duct cleaning device for tangential-longitudinal flow rice combine harvesters. Biosystems Engineering, 2019; 182: 98–106.
[33] Zhao L, Chen L Y, Yuan F, Wang L. Simulation study of rice cleaning based on DEM-CFD coupling method. Processes, 2022; 10(2): 281. doi: 10.3390/pr10020281.
[34] Yuan J B, Wu C Y, Li H, Qi X D, Xiao X X, Shi X X. Movement rules and screening characteristics of rice-threshed mixture separation through a cylinder sieve. Computers and Electronics in Agriculture, 2018; 154: 320–329.
[35] Luo C X, Jing S X, Han X M, Leng J F. Fluid-solid coupling field analysis of centrifugal fan based on nonlinear dynamics. Journal of Vibroengineering, 2017; 19(7): 5473–5481.